


Article

Effect of Revegetation in Extremely Degraded Grassland on Carbon Density in Alpine Permafrost Regions

Yinglan Jia ^{1,2}, Shengyun Chen ^{1,3,4,*}  and Peijie Wei ^{1,2}

¹ Cryosphere and Eco-Environment Research Station of Shule River Headwaters, State Key Laboratory of Cryospheric Science, Northwest Institute of Eco-Environment and Resources, Chinese Academy of Sciences, Lanzhou 730000, China

² University of Chinese Academy of Sciences, Beijing 100049, China

³ School of Geographical Sciences, Academy of Plateau Science and Sustainability, Qinghai Normal University, Xining 810008, China

⁴ Long-Term National Scientific Research Base of the Qilian Mountain National Park, Xining 810000, China

* Correspondence: sychen@lzb.ac.cn; Tel.: +86-931-4967316

Abstract: Revegetation has been proposed as an effective approach to restoring the extremely degraded grassland in the Qinghai–Tibetan Plateau (QTP). However, little is known about the effect of revegetation on ecosystem carbon density (ECD), especially in alpine permafrost regions. We compared aboveground biomass carbon density (ABCD), belowground biomass carbon density (BBCD), soil organic carbon density (SOC), and ECD in intact alpine meadow, extremely degraded, and revegetated grasslands, as well as their influencing factors. Our results indicated that (1) ABCD, BBCD, SOC, and ECD were significantly lower in extremely degraded grassland than in intact alpine meadow; (2) ABCD, SOC, and ECD in revegetated grassland significantly increased by 93.46%, 16.88%, and 19.22%, respectively; (3) stepwise regression indicated that BBCD was mainly influenced by soil special gravity, and SOC and ECD were controlled by freeze–thaw strength and soil temperature, respectively. This study provides a comprehensive survey of ECD and basic data for assessing ecosystem service functions in revegetated grassland of the alpine permafrost regions in the QTP.

Keywords: extremely degraded grassland; revegetated grassland; ecosystem carbon density; alpine permafrost regions



Citation: Jia, Y.; Chen, S.; Wei, P. Effect of Revegetation in Extremely Degraded Grassland on Carbon Density in Alpine Permafrost Regions. *Sustainability* **2022**, *14*, 12575. <https://doi.org/10.3390/su141912575>

Academic Editor: Teodor Rusu

Received: 24 August 2022

Accepted: 29 September 2022

Published: 3 October 2022

Publisher's Note: MDPI stays neutral with regard to jurisdictional claims in published maps and institutional affiliations.



Copyright: © 2022 by the authors. Licensee MDPI, Basel, Switzerland. This article is an open access article distributed under the terms and conditions of the Creative Commons Attribution (CC BY) license (<https://creativecommons.org/licenses/by/4.0/>).

1. Introduction

Ecosystem carbon storage is recognized to be an important indicator of ecological function [1], considering the role of the carbon cycle in maintaining a stable climate. It is the total amount of carbon stored in the terrestrial ecosystem and usually is the sum of four carbon components: aboveground biomass (AB), belowground biomass (BB), soil organic carbon (SOC), and litter [2]. The quantitative study of ecosystem carbon can provide basic reference data for the reasonable management of the grassland ecosystem and the sustainable use of natural resources [3].

Grassland is the key element of the terrestrial ecosystem and covers 37–50% of the terrestrial area of the world [4,5]. It stores approximately 34% of the global terrestrial stock of carbon and plays a major role as a sink of atmospheric carbon [6]. In recent decades, about 49.25% of the world's grassland has experienced degradation due to climate change and anthropogenic activities [7]. It has been estimated that approximately 7.51 Tg (1 Tg = 10¹² g) of vegetation carbon and 4050 Tg of SOC in degraded grassland have been lost, respectively [7,8]. As a major soil carbon reservoir, permafrost stores vast amounts of SOC [9] due to its low temperature and slow decomposition rate. The Qinghai–Tibetan Plateau (QTP) has the largest permafrost cover among the mid- and low-latitude regions of the world [10]. Alpine grassland is the main vegetation type distributed in the permafrost

regions of the QTP [11], performing important ecosystem service functions, such as carbon storage [12]. However, approximately 90% of alpine grassland has been degraded, and approximately 35% of it has developed into extremely degraded grassland [13,14]. This has led to a decline not only in vegetation productivity but also in soil quality, further resulting in a decline in ecosystem service functions [15]. Therefore, it is essential to take measures to slow down and restore extremely degraded grasslands.

Revegetation in extremely degraded grasslands using cultivated grasses is a fast and effective approach, which has been widely applied in the QTP [16–19]. Previous studies have examined the carbon dynamics of vegetation or soil after revegetation. For example, revegetation significantly increases the aboveground and belowground biomass according to Li et al. [17]. Li et al. [20] found that the carbon storage in aboveground, belowground, and total biomass was significantly improved. Feng et al. [21] reported that SOC in the 0–10 cm layer increased by 13% after 3 years of revegetation. Bai et al. [19] also suggested that revegetation could increase the stability of SOC. Furthermore, some studies explored the factors influencing carbon storage, showing that soil texture and hydrothermal conditions are important, but that the degree and direction of their influence varied according to the geographical distribution and time scale. However, these studies mentioned above examined the role of soil or vegetation in carbon storage and even mostly concentrated on seasonally frozen regions. Despite this, fewer studies have attempted to quantify ecosystem carbon density (ECD) after revegetation, especially in alpine permafrost regions. Therefore, we hypothesized that (i) revegetation would improve the ECD of extremely degraded grassland; (ii) freeze–thaw strength might play a more important role in regulating ECD, compared with other environmental variables, such as soil texture and hydrothermal conditions in the permafrost regions of the QTP.

To validate these hypotheses, we selected the Shule River headwaters in the north-eastern margin of the QTP as the study area, where alpine permafrost develops widely, occupying about 97.98% of the total area. In the past decades, alpine grassland in this region also suffered significant degradation due to climate warming, overgrazing, and permafrost degradation [22–24], resulting in significant changes in the vegetation and soil environment. There was no doubt that ecosystem carbon was affected [25]. In this study, we investigated 9 plots and collected 45 soil samples from extremely degraded grassland, 4-year revegetated grassland, and intact alpine meadow. The objectives were to (1) assess the effects of degradation and revegetation on aboveground biomass carbon density (ABCD), belowground biomass carbon density (BBCD), soil organic carbon density (SOC), and ECD, (2) examine their influencing factors by employing regression analysis. Our results can provide a scientific reference for the restoration of extremely degraded grassland and the assessment of ecosystem service functions in revegetated grassland of the alpine permafrost regions in the QTP.

2. Materials and Methods

2.1. Study Area and Sampling Site

The study area is located in the Shule River headwaters in the western part of the Qilian Mountains (96.2°~99.0° E, 38.2°~40.0° N, and 3405~5827 m above sea level), northeast margin of the QTP, China (Figure 1). The total area is 4932.76 km² and is characterized by a continental arid desert climate, with a low annual mean air temperature from −2.1 to −7.4 °C and precipitation from 360 to 600 mm [26]. This area belongs to the alpine ecosystem [27] and widely develops alpine permafrost. Alpine grassland in this area has been degraded over the past few decades [22]. Thus, a comprehensive ecosystem observation field was established in July 2014. Meanwhile, we selected around 500 acres of the surrounding area in which to sow seeds of local grasses. Before seeding, the soil was plowed to a depth of 20 cm, and 10 kg ha^{−1} of chemical fertilizer (diammonium phosphate) was applied. Revegetation completely excluded livestock grazing by fencing. Therefore, we chose an area inside the fence as a revegetated grassland site and an area outside the fence as an extremely degraded grassland site. In addition, an area of intact alpine

meadow was selected as the control site. The description of the sampling sites was shown in Table 1. Mean annual air temperature and annual precipitation were calculated based on meteorological data of the observational sites in 2018.

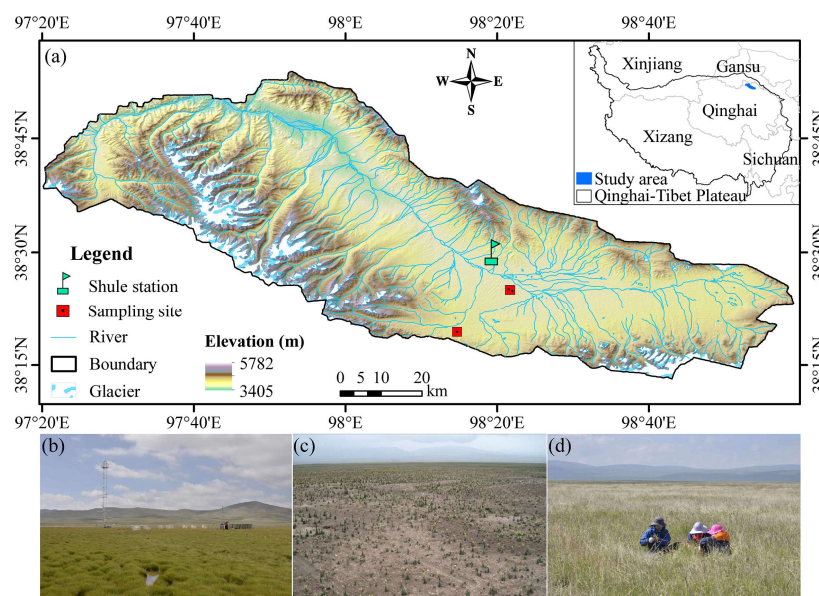


Figure 1. Location of the spatial distribution of the sampling sites in the study area (a) including intact alpine meadow (b), extremely degraded grassland (c), and revegetated grassland (d).

Table 1. Description of the sampling sites.

	IM	DG	RG
Longitude (E)	98°13'44''	98°22'01''	98°22'08''
Latitude (N)	38°19'58''	38°25'07''	38°25'35''
Elevation (m)	4036	3859	3859
Mean annual air temperature (°C)	−1.13	−4.16	−4.16
Annual precipitation (mm)	467	475	475
Coverage (%)	80	13	65
Dominant species	<i>Kobresia pygmaea</i> , <i>Kobresia tibetica</i>	<i>Aconitum pendulum</i> , <i>Artemisia nanschanica</i> , <i>Polygnum sibiricum</i>	<i>Elymus nutans</i> , <i>Festuca sinensis</i> , <i>Poa crymophila</i> , <i>Poa pratensis</i>

Note: IM: intact alpine meadow; DG: extremely degraded grassland; RG: revegetated grassland.

2.2. Sampling and Analysis Processes

At the end of July 2018, we randomly selected three quadrats (0.5 m × 0.5 m) in each site approximately 10 m away from each other to avoid the edge effect. AB was harvested in the quadrats, including green plants, litter, and dead tissue. BB was measured by mixing 5 soil cores (4.8-cm diameter), collecting the samples from 0–50 cm layers (divided into 5 layers, each layer being 10 cm deep) and passing them through a 2 mm sieve to remove impurities. All AB and BB samples were immediately dried at 80 °C until they reached a constant weight. Subsequently, soil samples from the 0–50 cm layers were collected with a soil auger (3.8 cm diameter) from each quadrat; the sampling method used was the same as that for BB. For fresh soil saved at 4 °C, the soil pH was determined by a PHBJ–260 pH meter (INESA, Shanghai, China), with a water ratio of 1:5. Using air-dried soils, SOC was measured using the Walkley–Black dichromate oxidation method (Nelson and Sommers, 1996). The soil specific gravity was measured by using a pycnometer. For the soil hydrothermal conditions, soil temperature, and moisture in the depths of 2 cm, 10 cm, 20 cm, 30 cm, and 40 cm below the soil surface were obtained by Hydra Probe II soil sensors (Stevens, USA) connected to a CR1000X datalogger (Campbell Scientific, Logan, UT, USA), with values being automatically recorded every 10 min.

2.3. Date Analysis

Based on soil temperature data, we classified the soil freeze–thaw processes for different grassland types. Firstly, the soil freeze–thaw processes included four stages, namely, a completely frozen stage, a thawing stage, a completely thawed stage, and a freezing stage. A detailed explanation can be found in Chen et al. [28]. Moreover, the duration of the completely thawed, completely frozen, and freeze–thaw stages was calculated [28]. Lastly, the calculation of freeze–thaw strength was conducted as suggested by Wu [29].

ABCD and BBCD were transformed considering a ratio of 0.475 [3]. SOCD was calculated as follows [3]:

$$\text{SOCD} = \sum_i^n h_i \times BD_i \times \text{SOC}_i \times (1 - C_i) / 100 \quad (1)$$

where h_i , BD_i , SOC_i , and C_i are the soil thickness (cm), bulk density ($\text{g}\cdot\text{cm}^{-3}$), soil organic carbon ($\text{g}\cdot\text{kg}^{-2}$), and volume percentage of the soil particle fraction of >2 mm in layer i , respectively. Additionally, $i = 1$ (0–10 cm), 2 (10–20 cm), 3 (20–30 cm), 4 (30–40 cm), and 5 (40–50 cm). The bulk density was estimated using the equation created by Yang et al. [30]. ECD was determined as the sum of ABCD, BBCD, and SOCD.

One-way analysis of variance (ANOVA) and the least significant difference (LSD) test were used to examine the significant differences in ABCD, BBCD, SOCD, and ECD among the different grassland types and soil layers with SPSS 22.0. Then, we used the random forest algorithm to determine the relative importance of environmental variables (soil temperature and moisture, specific gravity, freeze–thaw strength, and pH) for the components of carbon density (ABCD, BBCD, SOCD, and ECD). Pearson correlation was used to calculate the correlation coefficient between the components of carbon density and environmental variables. Finally, stepwise regression was used to explore the relationships between the different of carbon densities and environmental variables. All pictures were generated using the “ggplot2” packages of R 3.6.3.

3. Results

3.1. Environmental Variables

3.1.1. Soil Physicochemical Properties

Soil temperature, moisture, pH, specific gravity, and freeze–thaw strength were presented in Table 2. The soil temperature in extremely degraded grassland was significantly higher than in intact alpine meadow and revegetated grassland ($p < 0.05$), while it was not significantly different in the latter two grasslands ($p > 0.05$). The largest values of soil moisture and freeze–thaw strength were found in intact alpine grassland, followed by extremely degraded grassland and revegetated grassland, and there was a significant difference in soil moisture among the three types of grassland ($p < 0.05$), but the differences in freeze–thaw strength were insignificant ($p > 0.05$). We found that pH was statistically insignificantly ($p > 0.05$) higher in extremely degraded grassland than in intact alpine meadow and revegetated grassland.

Table 2. Soil physicochemical properties in intact alpine meadow (IM), extremely degraded grassland (DG), and revegetated grassland (RG) in the 0–50 cm depths (mean \pm SE).

	IM	DG	RG
Soil temperature ($\text{g}\cdot\text{cm}^{-3}$)	6.526 \pm 1.177 ^b	12.842 \pm 2.444 ^a	9.494 \pm 0.839 ^b
Soil moisture (%)	49.362 \pm 1.646 ^a	37.740 \pm 2.569 ^b	33.820 \pm 3.079 ^c
Soil specific gravity ($\text{g}\cdot\text{cm}^{-3}$)	2.316 \pm 0.063 ^b	2.637 \pm 0.013 ^a	2.636 \pm 0.010 ^a
pH	8.106 \pm 0.043 ^a	8.061 \pm 0.109 ^a	8.107 \pm 0.042 ^a
Freeze–thaw strength (10^{-4})	32.042 \pm 29.654 ^a	8.676 \pm 8.548 ^a	3.140 \pm 1.790 ^a

Note: Different lowercase letters indicate significant differences between sample sites at the level of 0.05.

3.1.2. Soil Freeze–Thaw Characteristics

The seasonal dynamics of soil freeze–thaw processes for different types of grassland were shown in Figure 2. Compared with intact alpine meadow, degradation delayed the starting dates and advanced the ending dates of the completely frozen stage and freezing stage, with an average delay of 22 days and 25 days, as well as advances of 28 days and 2 days, respectively (Figure 2a,b). Degradation tended to advance the starting dates of the completely thawed and thawing stages as well as the ending dates of the thawing stage but delayed the ending date of the completely thawed stage, with average advances of 37 days, 29 days, and 9 days, as well as a delay of 61 days, respectively (Figure 2a,b). In contrast, compared with the extremely degraded grassland, revegetation advanced the starting dates of the completely frozen stage and freezing stage as well as the ending dates of the freezing stage, but delayed the ending date of the completely frozen stage, with an average advance of 25 days, 22 days, and 4 days and a delay of 39 days, respectively (Figure 2b,c). Revegetation delayed the starting dates and advanced the ending dates of the completely thawed and thawing stages, with an average delay of 36 days and 40 days, as well as advances of 56 days and 4 days, respectively (Figure 2b,c). Thus, degradation extended the duration of the completely thawed stage and shortened the duration of the completely frozen stage. Revegetation showed the opposite trend, that is, it extended the duration of the completely frozen stage and shortened the duration of the completely thawed stage. Especially, degradation increased duration of the completely thawed stage by 62 days ($p < 0.05$) and decreased the duration of the completely frozen and freeze–thaw stages by 51 days ($p < 0.05$) and 11 days, respectively. Additionally, revegetation in degraded grassland increased the duration of the completely frozen stage by 58 days ($p < 0.05$) and decreased the duration of the completely thawed and freeze–thaw stages by 53 days ($p < 0.05$) and 5 days, respectively. In addition, the duration of the completely frozen and completely thawed stages in the revegetated grassland were 7 days and 9 days longer than in the intact alpine meadow, respectively.

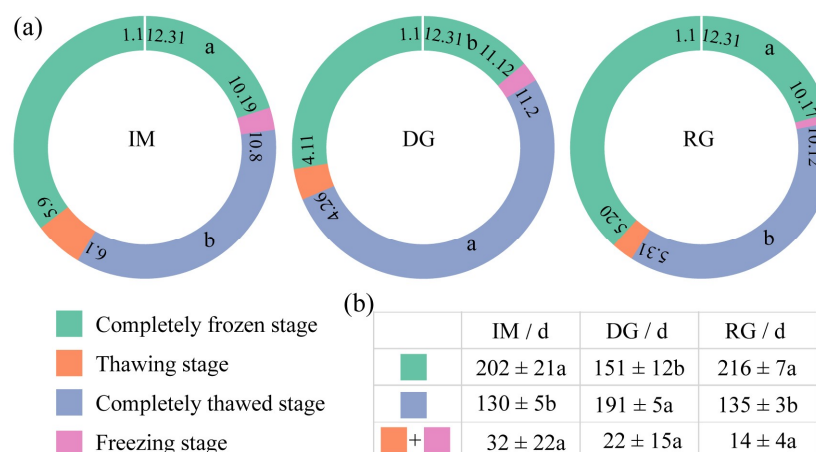


Figure 2. Soil freeze–thaw processes in intact alpine meadow (IM), extremely degraded alpine grassland (DG), and revegetated grassland (RG). The starting and ending dates of different stages (a), number of days in the completely frozen, completely thawed, and freeze–thaw stages (b). The numbers in the ring are time nodes (e.g., 1.1 means 1 January). Different lowercase letters indicate significant differences between sample sites at the level of 0.05.

3.2. Carbon Density

3.2.1. Variations in Aboveground and Belowground Biomass Carbon Densities

There was a significant change after revegetation in ABCD ($p < 0.05$, Figure 3a). From intact alpine meadow to extremely degraded grassland to revegetated grassland, ABCD first decreased and then increased, with revegetated grassland having the largest ABCD ($131.16 \text{ g} \cdot \text{m}^{-2}$). Compared with intact alpine meadow, ABCD decreased by 78.04% in

extremely degraded grassland. ABCD in revegetated grassland improved, being 93.46% and 780.85% higher than in intact alpine meadow and extremely degraded grassland, respectively. A significant difference was measured between extremely degraded grassland and revegetated grassland ($p < 0.05$).

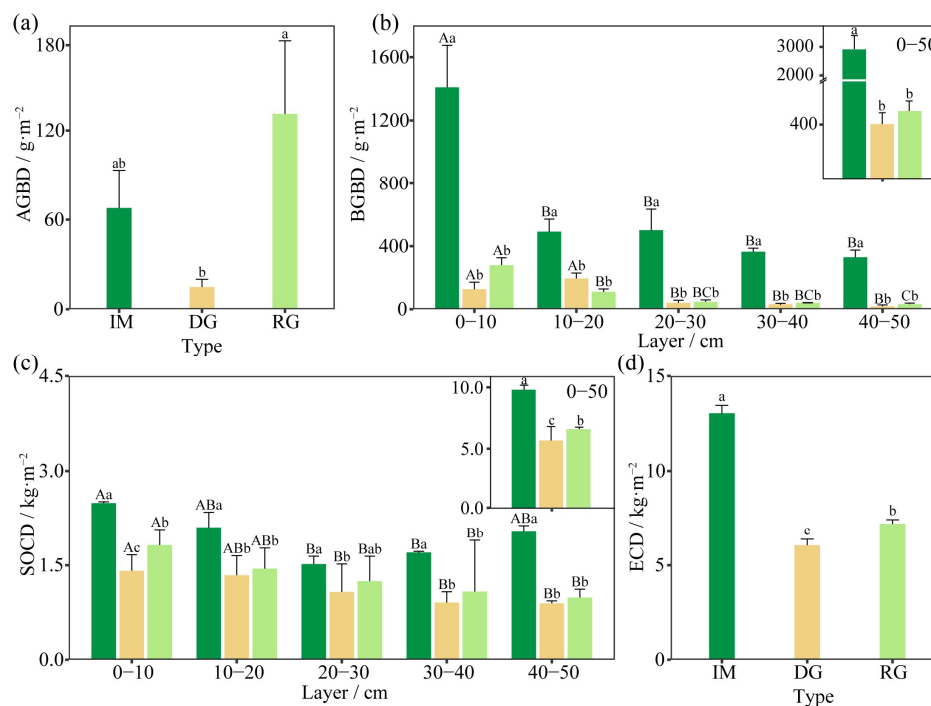


Figure 3. Variations in the different carbon densities in intact alpine meadow (IM), extremely degraded alpine grassland (DG), and revegetated grassland (RG). Aboveground biomass carbon density (a), belowground biomass carbon density (b), soil organic carbon density (c), and ecosystem carbon density (d). Different lowercase and capital letters indicate significant differences among sample sites and soil layers in the same grassland at the level of 0.05, respectively.

Grassland degradation significantly reduced BBCD ($p < 0.05$, Figure 3b). The average BBCD in the 0–50 cm layer in intact alpine meadow was $3096.71 \text{ g} \cdot \text{m}^{-2}$, which was significantly higher than that in extremely degraded grassland ($413.20 \text{ g} \cdot \text{m}^{-2}$) and revegetated grassland ($511.27 \text{ g} \cdot \text{m}^{-2}$). Specifically, 86.66% of BBCD was lost due to grassland degradation, but only 23.73% of BBCD increased after revegetation. The trends of BBCD variations in the layers of 0–10, 10–20, 20–30, 30–40, and 40–50 cm in the three sites were the same as those in the 0–50 cm layer, except for the 10–20 cm layer. A difference was observed between extremely degraded grassland and revegetated grassland, namely, the BBCD in extremely degraded grassland was higher than that in revegetated grassland. In addition, the distribution of BBCD varied significantly with soil (Table 3), with a decreasing trend seen throughout the soil depth in different types of grassland. The range of BBCD variation in intact alpine meadow, extremely degraded grassland, and revegetated grassland was $329.70\text{--}1409.45 \text{ g} \cdot \text{m}^{-2}$, $18.24\text{--}194.58 \text{ g} \cdot \text{m}^{-2}$, and $32.54\text{--}279.79 \text{ g} \cdot \text{m}^{-2}$, respectively. The BBCD in the 0–10 cm layer was higher than that in the 20–50 cm layers in both intact alpine meadow and revegetated grassland ($p < 0.05$), while the BBCD in the 0–20 cm layer was higher than that in the 30–50 cm layer in extremely degraded grassland ($p < 0.05$). In addition, the BBCD in intact alpine meadow, extremely degraded grassland, and restored grassland accounted for 97.89%, 96.71%, and 81.27% of the total vegetation carbon density, respectively.

Table 3. Results of two-way ANOVA (analysis) of the effects of soil layer and grassland type on aboveground biomass carbon density (ABCD), belowground biomass carbon density (BBCD), soil organic carbon density (SOCD), and ecosystem carbon density (ECD).

Factor	ABCD			BBCD			SOCD			ECD		
	<i>df</i>	<i>F</i>	<i>p</i>	<i>df</i>	<i>F</i>	<i>p</i>	<i>df</i>	<i>F</i>	<i>p</i>	<i>df</i>	<i>F</i>	<i>p</i>
Layer	-	-	-	4	16.785	< 0.001	4	22.899	< 0.001	-	-	-
type	2	3.340	0.106	2	67.424	< 0.001	2	89.929	< 0.001	2	148.217	< 0.001
Layer × type	-	-	-	8	7.428	< 0.001	8	2.658	0.025	-	-	-

Note: *df* is the degree of freedom, *F* is the statistic, and *p* is the value that is judged to be significant.

3.2.2. Change in Soil Organic Carbon Density

As shown in Figure 3c, SOCD was significantly affected by grassland degradation and revegetation ($p < 0.05$). In the layer of 0–50 cm in intact alpine meadow, SOCD ($9.87 \text{ kg} \cdot \text{m}^{-2}$) was higher than in extremely degraded grassland ($5.63 \text{ kg} \cdot \text{m}^{-2}$) and revegetated grassland ($6.58 \text{ kg} \cdot \text{m}^{-2}$). SOCD in extremely degraded grassland decreased by 43.00% compared with that in intact alpine meadow and increased by 16.88% in revegetated grassland compared with that in extremely degraded grassland. Similarly, the trend of SOCD in each soil layer was the same as that in the 0–50 cm layer, and a significant difference was observed in the 0–10 cm layer between extremely degraded grassland and revegetated grassland. As regards the profile change, SOCD in extremely degraded grassland and revegetated grassland showed a gradual trend of decrease, and the value in the 0–10 cm layers was higher than that in the 20–50 cm layers ($p < 0.05$). However, SOCD in the intact alpine meadow showed a “V”-shaped change and reached a minimum value in the 20–30 cm layer; the value in the 0–10 cm layer was higher than that in the 20–40 cm layers ($p < 0.05$).

3.2.3. Variation in Ecosystem Carbon Density

The ECD declined from intact alpine meadow ($13.04 \pm 0.41 \text{ kg} \cdot \text{m}^{-2}$) to revegetated grassland ($7.22 \pm 0.21 \text{ kg} \cdot \text{m}^{-2}$) to extremely degraded grassland ($6.05 \pm 0.33 \text{ kg} \cdot \text{m}^{-2}$), and there was a significant difference among the different types of grassland (Figure 3d). The ECD in extremely degraded grassland decreased by 53.55% compared with that in intact alpine meadow and increased by 19.22% after revegetation ($p < 0.05$).

3.3. Factors Influencing Carbon Density

Two-way ANOVA revealed that the types of grassland insignificantly affected the ABCD (Table 3, $p > 0.05$). Soil layers, grassland types, and their interaction had a significant impact on both BBCD and SOCD ($p < 0.05$). The types of grassland significantly affected ECD ($p < 0.001$). The relative importance of predictor variations is shown in Figure 4. For ABCD, pH ranked first in importance, followed by freeze–thaw strength, soil temperature, moisture, and soil specific gravity. In contrast, the importance of pH for BBCD, SOCD, and ECD was relatively small. For BBCD, the difference in importance between freeze–thaw strength, soil specific gravity, and soil moisture was small, and soil temperature showed even less importance. For SOCD, soil temperature ranked first in importance, and the difference in importance between soil moisture and freeze–thaw intensity was small; soil specific gravity was less important. For ECD, the factor of the greatest importance was freeze–thaw strength, followed by soil temperature, moisture, and, finally, soil specific gravity.

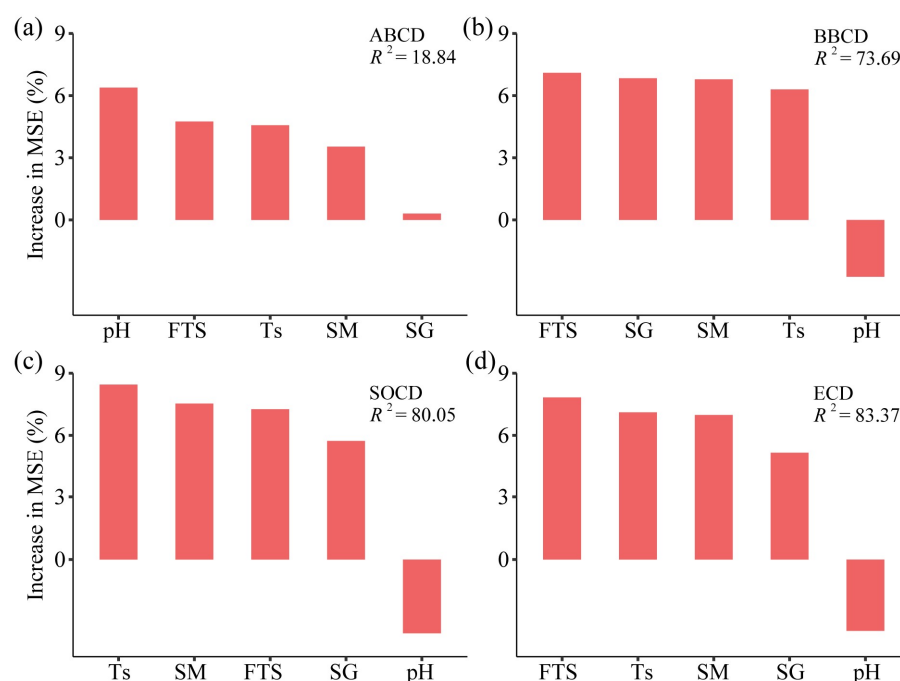


Figure 4. Relative importance of predictive variations in random forest models. FTS: freeze–thaw strength; Ts: soil temperature; SM: soil moisture; SG: soil specific gravity. Aboveground biomass carbon density (a), belowground biomass carbon density (b), soil organic carbon density (c), and ecosystem carbon density (d).

The results of Pearson correlation analysis are displayed in Figure 5. No significant correlation was found between ABCD and environmental variables. The BBBCD was significantly and negatively correlated with soil temperature and specific gravity ($p < 0.01$), and significantly and positively correlated with soil moisture and freeze–thaw strength ($p < 0.001$). Similar results were also observed for SOCD and ECD. In addition, soil moisture and freeze–thaw strength had a significant negative correlation with soil temperature and a significant positive correlation with specific gravity ($p < 0.05$). Additionally, soil moisture and freeze–thaw strength had a significant negative correlation with specific gravity ($p < 0.05$).

Using the standardized coefficients of stepwise linear regression (Table 4), the results indicated that BBBCD had a significantly negative relationship with soil specific gravity (standardized coefficient = -0.965 , $p < 0.001$) and explained 92.1% of the variation in BBBCD. SOCD was significantly and positively correlated with freeze–thaw strength (standardized coefficient = 0.481 , $p < 0.001$) but significantly negatively correlated with soil temperature (standardized coefficient = -0.587 , $p < 0.001$) in the linear equation. Overall, these factors explained 99.8% of the SOCD variation, and freeze–thaw strength was able to explain the greatest amount of variation. In addition, freeze–thaw strength (standardized coefficient = 0.575 , $p = 0.001$) exhibited a significantly positive relationship with ECD, and soil temperature (standardized coefficient = -0.486 , $p = 0.001$) showed a significant negative correlation with ECD, being able to explain 97.4% of its variation.

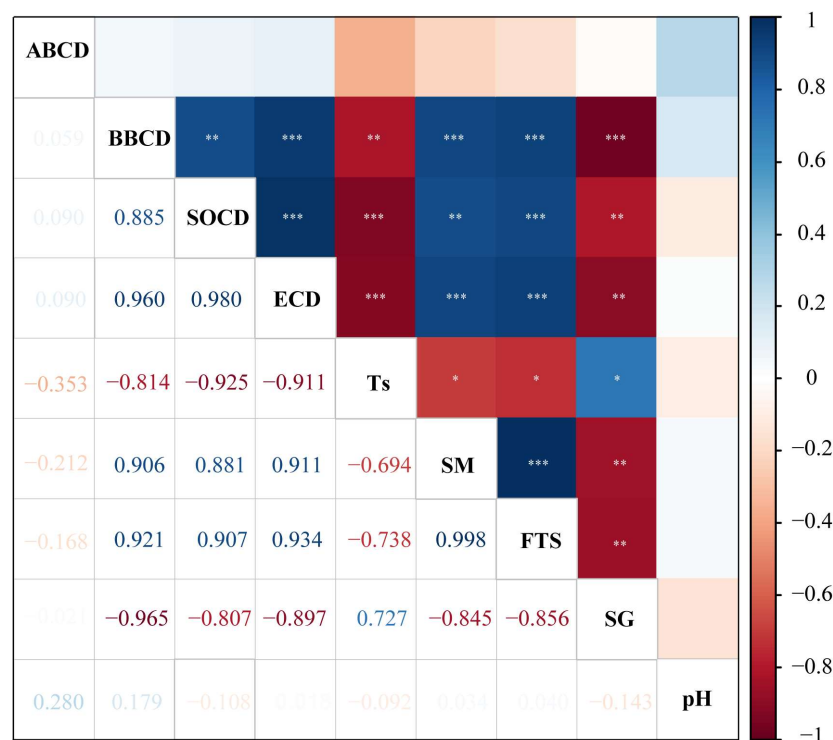


Figure 5. Heatmap of correlation (Pearson) between carbon density (ABCD, BBCD, SOCD, ECD) and environmental variables. Ts: soil temperature; SM: soil moisture; FTS: freeze–thaw strength; SG: soil specific gravity. * $p < 0.05$, ** $p < 0.01$, *** $p < 0.001$.

Table 4. Results from stepwise regressions of the different forms of carbon densities and environmental factors.

	Equation (standardized coefficients)	R ² _{adj}	p
ABCD	–	–	–
BBCD	BBCD = $-0.965 \times \text{SG}$	0.921	< 0.001
SOCD	SOCD = $-0.563 \times \text{Ts} + 0.492 \times \text{FTS}$	0.956	< 0.001
ECD	ECD = $0.575 \times \text{FTS} - 0.486 \times \text{Ts}$	0.974	< 0.001

4. Discussion

4.1. Degradation Decreased Carbon Density

Grassland degradation was often coupled with alterations in vegetation and soil [31], which resulted in a decrease in carbon storage. In recent years, many scholars have explored the dynamics of vegetation carbon density and SOCD due to grassland degradation. Among them, Li et al. [20] reported that the carbon density of plants, litter, and the belowground carbon density in Tianzhu County of the QTP decreased with increasing degradation levels and that more than 80% of carbon reduction can take place in extremely degraded grassland. Wen et al. [32] found that the SOCD of extremely degraded grassland was lower than that of intact alpine meadow in Maqin Country of the QTP, and Xu et al. [31] determined that the loss of SOC was concentrated in the 0–40 cm layer in Songnen Plain. Our results were consistent with the findings of these previous studies. We found that BBCD, SOCD, and ECD in extremely degraded grassland were significantly decreased by 86.66%, 43.00%, and 53.55% compared to those in intact alpine meadow, respectively. These decreases were mainly associated with reduced carbon input and increased erosion. On the one hand, aboveground and belowground biomasses, which were the main carbon input, significantly decreased as degradation progressed [20]; therefore, the lower vegetation productivity had a negative impact on carbon accumulation. On the other hand, soil erosion

in degraded grassland increased due to a lack of vegetation protection, including from water and wind erosion [33,34]. These were additional processes that accelerated carbon loss and cannot be ignored. In addition, the ABCD in extremely degraded grassland was insignificantly lower than that in intact alpine meadow. This was mainly due to an increase in the proportion of poisonous plants. Although these were species of a low use-value, they have high biomass and can gradually expand to become dominant in areas of grassland degradation [35].

4.2. Revegetation Improved Carbon Density

Revegetation in extremely degraded grassland has been thought to enhance the sustainability of the grassland ecosystem in the QTP [16]. In our study, the ABCD in revegetated grassland was significantly higher than in extremely degraded grassland and increased by about 780.85% in the Shule River headwaters, which was consistent with the findings of other studies [20,36]. Part of the reason for this can be the increase in the coverage and the inhibition of the fence. In the short term, the coverage of revegetation can be significantly improved [21]. Generally, fencing protected the palatable grasses and sedges that can produce more high-quality litter for decomposers, directly affecting the ABCD [37]. However, we did not observe a significant correlation between ABCD and environmental variables. This may be because the main factor influencing ABCD in this region was the meteorological factor. Several studies have shown that ABCD was significantly correlated with precipitation and air temperature [36,38] by regulating plant photosynthesis and further affecting carbon accumulation. In our study, the air temperature and precipitation in extremely degraded grassland and revegetated grassland were the same, so they could not be analyzed as environmental variables.

We found that the BBCD in revegetated grassland was insignificantly high compared with that in extremely degraded grassland and was negatively correlated with soil specific gravity. Specific gravity was an important soil grain property, which was known to be required in the computation of soil porosity [39]. As specific gravity increases, soil porosity increases, which can increase the oxygen content in the soil, promoting microbial activity and accelerating the mineralization of organic matter [40,41]. This, in turn, had a negative effect on BBCD. Interestingly, the BBCD in extremely degraded grassland in the 10–20 cm layer was higher than that in revegetated grassland (Figure 2), which can be explained considering the BAR. The BAR was the ratio of belowground biomass to aboveground biomass and can be used as an indicator of a plant community stability [42]. Zhang et al. [42] reported that an increased BAR directly influenced soil microbial biomass carbon and dissolvable organic carbon and indirectly enhanced vegetation carbon density. In our study, the BAR in extremely degraded grassland in the 10–20 cm layer was higher than in revegetated grassland (Table 5); this indicated that the root system of poisonous weeds (*Pedicularis kansuensis*, *Ligularia virgaurea*, and *Aconitum pendulum*) in degraded grassland was relatively stable in this layer. This also partly explains why the BBCD was not significantly increased.

Table 5. BAR in intact alpine meadow (IM), extremely degraded grassland (DG), and revegetated grassland (RG) in the 0–50 cm layers (mean \pm SE).

Site	0–10 cm	10–20 cm	20–30 cm	30–40 cm	40–50 cm
IM	6.70 \pm 3.77	2.34 \pm 1.15	2.38 \pm 1.91	1.73 \pm 0.33	1.57 \pm 0.65
DG	0.60 \pm 0.64	0.93 \pm 0.50	0.19 \pm 0.24	0.16 \pm 0.07	0.09 \pm 0.13
RG	1.33 \pm 0.66	0.53 \pm 0.25	0.22 \pm 0.18	0.19 \pm 0.01	0.15 \pm 0.09

SOCD was the result of carbon input from vegetation production and carbon output through decomposition and leaching [31]. Several studies have indicated the significant potential of revegetation to improve SOCD, reported that SOCD was strongly correlated with soil temperature, which was consistent with our results [43,44]. In alpine permafrost regions, a low soil temperature limited the decomposition of organic matter, which was one

of the main reasons for there being a large amount of SOCD [45]. Matzner and Borken [46] reported that the effect of the freeze–thaw process on carbon storage on an interannual scale was small; this was different from the results of this study. Our results showed that the freeze–thaw strength was positively correlated with SOCD. The freeze–thaw strength reflects the frequency and extent of daily freeze–thaw cycles, which were mainly related to soil microorganisms and moisture. Li et al. [47] reported that freeze–thaw cycles damaged the richness and diversity of bacteria, making it difficult to recover them to the original level, which slowed down the rate of decomposition of organic matter by microorganisms [48]. In addition, we found a significant correlation between freeze–thaw strength and soil moisture in the 0–30 cm layers (Figure 6) and chose these layers because the difference in freeze–thaw strength in grassland types was significant (data not shown). Soil moisture was closely related to permafrost and vegetation development [49,50], and a high soil moisture not only supported a high vegetation productivity but also affected the decomposition of organic matter by affected the soil redox reactions [50–52].

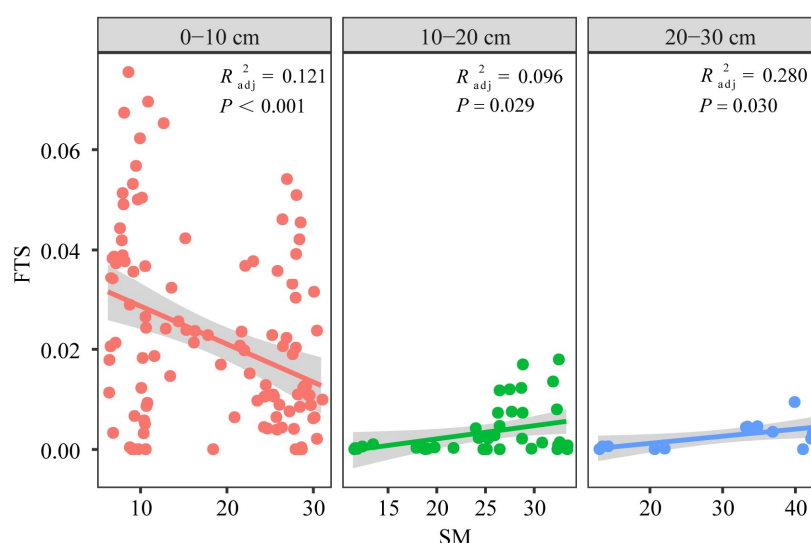


Figure 6. Comparisons of the soil moisture (SM) and freeze–thaw strength (FTS) at the depth of 0–30 cm. The lines are the regression equation, and the shaded areas represent the 95.0% confidence intervals of the regression equations.

Revegetation in extremely degraded grassland improved the ECD, which was consistent with the results of a previous study [53]. We found that freeze–thaw strength and soil temperature had a significant effect on the ECD; this was different from the findings of Liu et al. [25]. Potential explanations for the different results obtained include the following: (1) the change in the SOCD, because this represented the largest proportion of the ECD, and (2) the effect of permafrost stability on the ECD (we used freeze–thaw strength to reflect permafrost stability). Thus, freeze–thaw strength should be used as a basic and effective variable in studies or models of alpine permafrost stability.

5. Conclusions

Our findings suggested that the extremely degraded grassland examined in this study significantly reduced the ecosystem carbon density and accounted for 53.55% of the ecosystem carbon density, mainly due to a significant reduction in belowground biomass carbon density and soil organic carbon density. After revegetation, the ecosystem carbon density significantly increased by 19.22%, mainly due to a significant reduction in aboveground biomass carbon density and soil organic carbon density. This indicated that the revegetation of extremely degraded grassland in alpine permafrost regions was an effective approach to restoring and further improving the ecosystem service functions of grassland, including carbon storage. However, the key drivers affecting the different components of carbon

density were different. Soil specific gravity was the most critical controller of belowground biomass carbon density. For soil organic carbon density and ecosystem carbon density, freeze–thaw strength and soil temperature were the most important influencing factors; therefore, freeze–thaw strength should be considered a basic and effective variable for modeling or predicting carbon density changes in alpine permafrost regions in the future. These results can provide a scientific reference and data basis for the restoration of extremely degraded grassland in permafrost regions and allow us to assess the enhancement of ecosystem service functions in alpine grassland.

Author Contributions: Conceptualization, S.C.; methodology, Y.J.; validation, S.C.; formal analysis, Y.J. and P.W.; investigation, S.C., P.W. and Y.J.; resources, S.C.; data curation, S.C.; writing—original draft preparation, Y.J.; writing—review and editing, Y.J., P.W. and S.C.; supervision, S.C.; funding acquisition, S.C. All authors have read and agreed to the published version of the manuscript.

Funding: This research was funded by the National Natural Science Foundation of China (41871064), the National Key Research and Development Program of China (2019YFC0507404), the Qinghai Key R&D and Transformation Program (2020-SF-146), the Freedom Project of the State Key Laboratory of Cryospheric Science, Northwest Institute of Eco-Environment and Resources, Chinese Academy of Sciences (SKLCS-ZZ-2022), and the Qinghai Province High-level Innovative “Thousand Talents” Program.

Institutional Review Board Statement: Not applicable.

Informed Consent Statement: Not applicable.

Data Availability Statement: The datasets used and/or analyzed during the current study are available from the corresponding author upon reasonable request.

Conflicts of Interest: The authors declare no conflict of interest.

References

1. Zhao, M.; He, Z.; Du, J.; Chen, L.; Lin, P.; Fang, S. Assessing the effects of ecological engineering on carbon storage by linking the CA-Markov and InVEST models. *Ecol. Indic.* **2019**, *98*, 29–38. [\[CrossRef\]](#)
2. He, C.; Zhang, D.; Huang, Q.; Zhao, Y. Assessing the potential impacts of urban expansion on regional carbon storage by linking the LUSD-urban and InVEST models. *Environ. Model. Softw.* **2016**, *75*, 44–58. [\[CrossRef\]](#)
3. Wei, P.; Chen, S.; Wu, M.; Jia, Y.; Xu, H.; Liu, D. Increased Ecosystem Carbon Storage between 2001 and 2019 in the Northeastern Margin of the Qinghai-Tibet Plateau. *Remote Sens.* **2021**, *13*, 3986. [\[CrossRef\]](#)
4. O'Mara, F.P. The role of grasslands in food security and climate change. *Ann. Bot.* **2012**, *110*, 1263–1270. [\[CrossRef\]](#)
5. Haferkamp, M.R.; MacNeil, M.D. Grazing Effects on Carbon Dynamics in the Northern Mixed-Grass Prairie. *Environ. Manag.* **2004**, *33*, S462–S474. [\[CrossRef\]](#)
6. Cheng, J.; Wu, G.; Zhao, L.P.; Li, Y.; Li, W.; Cheng, J.M. Cumulative effects of 20-year exclusion of livestock grazing on above- and belowground biomass of typical steppe communities in arid areas of the Loess Plateau, China. *Plant Soil Environ.* **2018**, *57*, 40–44. [\[CrossRef\]](#)
7. Gang, C.; Zhou, W.; Chen, Y.; Wang, Z.; Sun, Z.; Li, J.; Qi, J.; Odeh, I. Quantitative assessment of the contributions of climate change and human activities on global grassland degradation. *Environ. Earth Sci.* **2014**, *72*, 4273–4282. [\[CrossRef\]](#)
8. Dlamini, P.; Chivenge, P.; Chaplot, V. Overgrazing decreases soil organic carbon stocks the most under dry climates and low soil pH: A meta-analysis shows. *Agric. Ecosyst. Environ.* **2016**, *221*, 258–269. [\[CrossRef\]](#)
9. Ding, J.; Chen, L.; Ji, C.; Hugelius, G.; Li, Y.; Liu, L.; Qin, S.; Zhang, B.; Yang, G.; Li, F.; et al. Decadal soil carbon accumulation across Tibetan permafrost regions. *Nat. Geosci.* **2017**, *10*, 420–425. [\[CrossRef\]](#)
10. Zou, D.; Zhao, L.; Sheng, Y.; Chen, J.; Hu, G.; Wu, T.; Wu, J.; Xie, C.; Wu, X.; Pang, Q.; et al. A new map of permafrost distribution on the Tibetan Plateau. *Cryosphere* **2017**, *11*, 2527–2542. [\[CrossRef\]](#)
11. Wang, Z.; Wang, Q.; Zhao, L.; Wu, X.; Yue, G.; Zou, D.; Nan, Z.; Liu, G.; Pang, Q.; Fang, H.; et al. Mapping the vegetation distribution of the permafrost zone on the Qinghai-Tibet Plateau. *J. Mt. Sci.* **2016**, *13*, 1035–1046. [\[CrossRef\]](#)
12. Fayiah, M.; Dong, S.K.; Khomera, S.W.; Rehman, S.A.U.; Yang, M.Y.; Xiao, J.N. Status and Challenges of Qinghai-Tibet Plateau's Grasslands: An Analysis of Causes, Mitigation Measures, and Way Forward. *Sustainability* **2020**, *12*, 1099. [\[CrossRef\]](#)
13. Dong, S.; Li, J.; Li, X.; Li, W.; Zhu, L.; Li, Y.; Ma, Y.; Shi, J.; Dong, Q.; Wang, Y. Application of design theory for restoring the “black beach” degraded rangeland at the headwater areas of the Qinghai-Tibetan Plateau. *Afr. J. Agric. Res.* **2010**, *5*, 3542–3552.
14. Dong, S.; Sherman, R. Enhancing the resilience of coupled human and natural systems of alpine rangelands on the Qinghai-Tibetan Plateau. *Rangel. J.* **2015**, *37*, I–III. [\[CrossRef\]](#)

15. Wang, X.; Dong, S.; Yang, B.; Li, Y.; Su, X. The effects of grassland degradation on plant diversity, primary productivity, and soil fertility in the alpine region of Asia's headwaters. *Environ. Monit. Assess.* **2014**, *186*, 6903–6917. [\[CrossRef\]](#)
16. Dong, S.; Shang, Z.; Gao, J.; Boone, R. Enhancing sustainability of grassland ecosystems through ecological restoration and grazing management in an era of climate change on Qinghai-Tibetan Plateau. *Agric. Ecosyst. Environ.* **2020**, *287*, 16. [\[CrossRef\]](#)
17. Li, Y.; Dong, S.; Li, W.; Wang, X.; Wu, Y. Soil carbon and nitrogen pools and their relationship to plant and soil dynamics of degraded and artificially restored grasslands of the Qinghai-Tibetan Plateau. *Geoderma* **2014**, *213*, 178–184. [\[CrossRef\]](#)
18. Gao, X.; Dong, S.; Xu, Y.; Wu, S.; Wu, X.; Zhang, X.; Zhi, Y.; Li, S.; Liu, S.; Li, Y.; et al. Resilience of revegetated grassland for restoring severely degraded alpine meadows is driven by plant and soil quality along recovery time: A case study from the Three-river Headwater Area of Qinghai-Tibetan Plateau. *Agric. Ecosyst. Environ.* **2019**, *279*, 169–177. [\[CrossRef\]](#)
19. Bai, Y.; Ma, L.; Degen, A.A.; Rafiq, M.K.; Kuzyakov, Y.; Zhao, J.; Zhang, R.; Zhang, T.; Wang, W.; Li, X.; et al. Long-term active restoration of extremely degraded alpine grassland accelerated turnover and increased stability of soil carbon. *Glob. Chang. Biol.* **2020**, *26*, 7217–7228. [\[CrossRef\]](#)
20. Li, W.; Wang, J.; Zhang, X.; Shi, S.; Cao, W. Effect of degradation and rebuilding of artificial grasslands on soil respiration and carbon and nitrogen pools on an alpine meadow of the Qinghai-Tibetan Plateau. *Ecol. Eng.* **2018**, *111*, 134–142.
21. Feng, R.; Long, R.; Shang, Z.; Ma, Y.; Dong, S.; Wang, Y. Establishment of *Elymus natans* improves soil quality of a heavily degraded alpine meadow in Qinghai-Tibetan Plateau, China. *Plant Soil* **2010**, *327*, 403–411. [\[CrossRef\]](#)
22. Chen, S.; Liu, W.; Qin, X.; Liu, Y.; Zhang, T.; Chen, K.; Hu, F.; Ren, J.; Qin, D. Response characteristics of vegetation and soil environment to permafrost degradation in the upstream regions of the Shule River Basin. *Environ. Res. Lett.* **2012**, *7*, 045406. [\[CrossRef\]](#)
23. Xie, X.; Yang, G.J.; Wang, Z.R.; Wang, J. Landscape pattern change in mountainous areas along an altitude gradient in the upper reaches of Shule River. *Chin. J. Ecol.* **2010**, *29*, 1420–1426.
24. Niu, L.; Ye, B.; Li, J.; Sheng, Y. Effect of permafrost degradation on hydrological processes in typical basins with various permafrost coverage in Western China. *Sci. China Earth Sci.* **2011**, *54*, 615–624. [\[CrossRef\]](#)
25. Liu, W.; Chen, S.; Liang, J.; Qin, X.; Kang, S.; Ren, J.; Qin, D. The effect of decreasing permafrost stability on ecosystem carbon in the northeastern margin of the Qinghai-Tibet Plateau. *Sci. Rep.* **2018**, *8*, 4172. [\[CrossRef\]](#)
26. Wu, M.; Xue, K.; Wei, P.; Jia, Y.; Zhang, Y.; Chen, S. Soil microbial distribution and assembly are related to vegetation biomass in the alpine permafrost regions of the Qinghai-Tibet Plateau. *Sci. Total Environ.* **2022**, *834*, 155259. [\[CrossRef\]](#)
27. Wu, M.; Chen, S.; Chen, J.; Xue, K.; Chen, S.; Wang, X.; Chen, T.; Kang, S.; Rui, J.; Thies, J.E.; et al. Reduced microbial stability in the active layer is associated with carbon loss under alpine permafrost degradation. *Proc. Natl. Acad. Sci. USA* **2021**, *118*, e2025321118. [\[CrossRef\]](#) [\[PubMed\]](#)
28. Chen, S.; Li, X.; Wu, T.; Xue, K.; Luo, D.; Wang, X.; Wu, Q.; Kang, S.; Zhou, H.; Wei, D. Soil thermal regime alteration under experimental warming in permafrost regions of the central Tibetan Plateau. *Geoderma* **2020**, *372*, 11. [\[CrossRef\]](#)
29. Wu, M. Effects of Permafrost Environmental Changes on Soil Microbial Communities in the Shule River Headwater Regions. Ph.D. Thesis, University of Chinese Academy of Sciences, Beijing, China, 2022.
30. Yang, Y.; Fang, J.; Smith, P.; Tang, Y.; Jin-Sheng, H.E. Changes in topsoil carbon stock in the Tibetan grasslands between the 1980s and 2004. *Glob. Chang. Biol.* **2009**, *15*, 2723–2729. [\[CrossRef\]](#)
31. Xu, T.; Zhang, M.; Ding, S.; Liu, B.; Chang, Q.; Zhao, X.; Wang, Y.; Wang, J.; Wang, L. Grassland degradation with saline-alkaline reduces more soil inorganic carbon than soil organic carbon storage. *Ecol. Indic.* **2021**, *131*, 108194. [\[CrossRef\]](#)
32. Li, W.; Dong, S.; Li, Y.; Li, X.; Shi, J.; Wang, Y.; Liu, D.; Ma, Y. Effect of Degradation Intensity on Grassland Ecosystem Services in the Alpine Region of Qinghai-Tibetan Plateau, China. *PLoS ONE* **2013**, *8*, e58432.
33. Li, F.; Kang, L.; Zhang, H.; Zhao, L.; Shirato, Y.; Taniyama, I. Changes in intensity of wind erosion at different stages of degradation development in grasslands of Inner Mongolia, China. *J. Arid. Environ.* **2005**, *62*, 567–585. [\[CrossRef\]](#)
34. Wang, S.; Zhang, S.; Lin, X.; Li, X.; Li, R.; Zhao, X.; Liu, M. Response of soil water and carbon storage to short-term grazing prohibition in arid and semi-arid grasslands of China. *J. Arid. Environ.* **2022**, *202*, 104754. [\[CrossRef\]](#)
35. Li, Y.; Dong, S.; Liu, S.; Wang, X.; Li, W.; Wu, Y. The interaction between poisonous plants and soil quality in response to grassland degradation in the alpine region of the Qinghai-Tibetan Plateau. *Plant Ecol.* **2014**, *215*, 809–819. [\[CrossRef\]](#)
36. Wang, P.; Heijmans, M.; Mommer, L.; van Ruijven, J.; Maximov, T.C.; Berendse, F. Belowground plant biomass allocation in tundra ecosystems and its relationship with temperature. *Environ. Res. Lett.* **2016**, *11*, 8. [\[CrossRef\]](#)
37. Li, Y.; Dong, S.; Wen, L.; Wang, X.; Wu, Y. The effects of fencing on carbon stocks in the degraded alpine grasslands of the Qinghai-Tibetan Plateau. *J. Environ. Manag.* **2013**, *128*, 393–399. [\[CrossRef\]](#)
38. Ding, L.; Li, Z.; Shen, B.; Wang, X.; Xu, D.; Yan, R.; Yan, Y.; Xin, X.; Xiao, J.; Li, M.; et al. Spatial patterns and driving factors of aboveground and belowground biomass over the eastern Eurasian steppe. *Sci. Total Environ.* **2022**, *803*, 149700. [\[CrossRef\]](#)
39. Prakash, K.; Sridharan, A.; Thejas, H.K.; Swaroop, H.M. A Simplified Approach of Determining the Specific Gravity of Soil Solids. *Geotech. Geol. Eng.* **2012**, *30*, 1063–1067. [\[CrossRef\]](#)
40. Xu, Z.; Yu, G.; Zhang, X.; Ge, J.; He, N.; Wang, Q.; Wang, D. The variations in soil microbial communities, enzyme activities and their relationships with soil organic matter decomposition along the northern slope of Changbai Mountain. *Appl. Soil Ecol.* **2015**, *86*, 19–29. [\[CrossRef\]](#)
41. Yang, C.; Liu, J.; Ying, H.; Lu, S. Soil pore structure changes induced by biochar affect microbial diversity and community structure in an Ultisol. *Soil Tillage Res.* **2022**, *224*, 105505. [\[CrossRef\]](#)

42. Zhang, R.; Bai, Y.; Zhang, T.; Henkin, Z.; Degen, A.A.; Jia, T.; Guo, C.; Long, R.; Shang, Z. Driving Factors That Reduce Soil Carbon, Sugar, and Microbial Biomass in Degraded Alpine Grasslands. *Rangel. Ecol. Manag.* **2019**, *72*, 396–404. [[CrossRef](#)]
43. Bi, X.; Li, B.; Nan, B.; Fan, Y.; Fu, Q.; Zhang, X.S. Characteristics of soil organic carbon and total nitrogen under various grassland types along a transect in a mountain-basin system in Xinjiang, China. *J. Arid Land* **2018**, *10*, 612–627. [[CrossRef](#)]
44. Balasubramanian, D.; Zhou, W.; Ji, H.; Grace, J.; Bai, X.L.; Song, Q.; Liu, Y.; Sha, L.; Fei, X.; Zhang, X.; et al. Environmental and management controls of soil carbon storage in grasslands of southwestern China. *J. Environ. Manag.* **2020**, *254*, 10. [[CrossRef](#)] [[PubMed](#)]
45. Yuan, Z.; Jiang, X. Vegetation and soil covariation, not grazing exclusion, control soil organic carbon and nitrogen in density fractions of alpine meadows in a Tibetan permafrost region. *Catena* **2021**, *196*, 9. [[CrossRef](#)]
46. Matzner, E.; Borken, W. Do freeze–thaw events enhance C and N losses from soils of different ecosystems? A review. *Eur. J. Soil Sci.* **2008**, *59*, 274–284. [[CrossRef](#)]
47. Li, Y.; Wang, L.; Tian, L.; Zheng, H.; Ou, Y.; Yan, B.; Cui, H.; Bao, M.; Zhang, S.; Guan, F. Dissolved organic carbon, an indicator of soil bacterial succession in restored wetland under freeze–thaw cycle. *Ecol. Eng.* **2022**, *177*, 106569. [[CrossRef](#)]
48. Schimel, J.P.; Clein, J. Microbial response to freeze–thaw cycles in tundra and taiga soils. *Soil Biol. Biochem.* **1996**, *28*, 1061–1066. [[CrossRef](#)]
49. Ping, C.-L.; Jastrow, J.; Jorgenson, M.; Michaelson, G.; Shur, Y. Permafrost soils and carbon cycling. *Soil* **2015**, *1*, 147–171. [[CrossRef](#)]
50. Wu, X.; Zhao, L.; Hu, G.; Liu, G.; Li, W.; Ding, Y. Permafrost and land cover as controlling factors for light fraction organic matter on the southern Qinghai-Tibetan plateau. *Sci. Total Environ.* **2018**, *613–614*, 1165–1174. [[CrossRef](#)]
51. Garten, C.; Hanson, P. Measured forest soil C stocks and estimated turnover times along an elevation gradient. *Geoderma* **2006**, *136*, 342–352. [[CrossRef](#)]
52. Peng, F.; Xue, X.; You, Q.; Huang, C.; Dong, S.; Liao, J.; Duan, H.; Tsunekawa, A.; Wang, T. Changes of soil properties regulate the soil organic carbon loss with grassland degradation on the Qinghai-Tibet Plateau. *Ecol. Indic.* **2018**, *93*, 572–580. [[CrossRef](#)]
53. Yuan, J.; Ouyang, Z.; Zheng, H.; Su, Y. Ecosystem carbon storage following different approaches to grassland restoration in south-eastern Horqin Sandy Land, northern China. *Glob. Ecol. Conserv.* **2021**, *26*, e01438. [[CrossRef](#)]